universität wien

MASTERARBEIT | MASTER'S THESIS

Titel | Title

Cell geometry of border and central cell in metal-grown Physcomitrium patens

verfasst von | submitted by

Jorge Luis Posada Corona

angestrebter akademischer Grad | in partial fulfilment of the requirements for the degree of

Master of Science (MSc)

Wien | Vienna, 2026

Studienkennzahl lt. Studienblatt | Degree programme code as it appears on the student record sheet:	UA 066 832
Studienrichtung lt. Studienblatt | Degree programme as it appears on the student record sheet:	Masterstudium Botany
Betreut von | Supervisor:	ao. Univ.-Prof. Mag. Dr. Ingeborg Lang Privatdoz.

ZUSSAMMENFASSUNG

Die Bryophyten umfassen drei verschiedene Untergruppen: Laubmoose, Lebermoose und Hornmoose. Bei Bryophyten beginnt die Entwicklung mit der Spezifikation der Blatt-Anfangszelle, die ein meristematisches Potential behält und Tochterzellen entstehen. Es gibt einen ausgeprägten morphologischen Unterschied zwischen jungen und reifen Blättern in *P. patens*. Die Hauptunterschiede hängen von Formänderungen ab: 1) der Randzellen (länger, schmaler und mit marginalen Verzahnungen) und 2) einer mehrzelligen Mittelrippe. Wie bei Angiospermen benötigt auch *P. patens* Makronährstoffe (N, P, S, K, Ca & Mg) in höheren Konzentrationen zwischen 0.1µM bis 1M (N) und Mikronährstoffe (Fe, Mn, B, Zn, Cu, Mo, Cl & Ni) in höheren Konzentrationen zwischen 0.1 bis 45µM zum Wachsen. In dieser Arbeit wollten wir die morphologischen Veränderungen untersuchen, die zwei Mikronährstoffe (Fe und Cu) in der Entwicklung der *P. patens*-Blättchen auslösen können. Dazu kultivierten wir *P. patens* unter 4 verschiedenen Bedingungen (Kontrolle, Fe, Cu und Fe&Cu) und analysierten Länge, Breite und Zellwanddicke der Zellen, die die Blättchen zusammensetzen, unter dem konfokalen Laserscanning-Mikroskop, indem wir die Zellwand mit Calcofluor White anfärbten. Wir fanden nichts statistisch signifikante Unterschiede zwischen alles Variablen für die 4 Grupen. die Randzellen waren statistisch signifikant länger und schmaler als die Zentralzellen, nur ins Iron und Copper Gruppen. Für die Zellwanddicke zeigt der signifikante Unterschied, der bei der Eisen-Kupfer-Gruppe gefunden wurde. Unsere Abschluss ist dass es mehr morphologische Unterschiede gibt, zusätzlich zu den in der Literatur berichteten (Länge und Breite), die zwischen den 2 Blattelltypen noch unentdeckt sind.

ABSTRACT

The bryophytes comprise three distinct subgroups: mosses, liverworts, and hornworts. In bryophytes, development starts with the specification of the leaf initial cell, the one keeps a meristematic potential and originates daughter cells. There is a distinguished morphological difference between young and mature leaves in *P. patens*. The main differences rely on shape changes: 1) of the border cells (longer, narrower and with marginal serrations), and 2) a multicellular midrib. Similarly to angiosperms, *P. patens* requires macronutrients (N, P, S, K, Ca & Mg) in concentrations ranging from 0.1µM to 1M (N) and micronutrients (Fe, Mn, B, Zn, Cu, Mo, Cl, Na, Co & Ni) in concentrations ranging from 0.1 to 45µM. In this work, we wanted to explore the morphological changes that 2 micronutrients (Fe and Cu) can trigger in the development of the *P. patens* leaf. To achieve this, we cultured *P. patens* under 4 different conditions (control, Fe, Cu and Fe&Cu) and analyzed the length, width and cell wall thickness of the cells composing the leaves under confocal laser scanning microscope by staining (with calcofluor white) the cell wall. We did not find statistically significant differences, for the 3 variables, among the 4 conditions. Border cells were statistically significantly longer and narrower than central cells, only in the iron and copper groups. For cell wall thickness, the only significant difference was found in the ironcopper group. We conclude that there are more morphological differences, in addition to the reported in the literature (length and width), to be unrevealed between the 2 leaf cell types.

ACKNOWLEDGMENTS

First, I would like to thank my mother, father, sister, and grandmother from the bottom of my heart for their unconditional support and love, because without it I would not have been able to go through this journey. Next, I want to thank my supervisor, Dr. Ingeborg Lang, for whom I am specially grateful for the trust and freedom given to me to do research in the university facilities. I also thank PhD Luigi Schillaci who also helped me through the whole research. The author also thanks all members of the Lang group and the people who helped me in the MOSYS department. Special thanks to the Core Facility Cell Imaging and Ultrastructure Research of University of Vienna - member of the Vienna Life-Science Instruments (VLSI) - who taught, and gave me access to the operation of the confocal microscope. I would like to thank to all the teachers I have met during all the subjects taken, because the sum of all have made me understand better the major parts of land plant biology. Last but not least, I would like to express my sincere gratitude to all the new friends that I have made during these 2 years and for all their support, learning and joys shared during all this time.

Thank you all!

Contents

1 Introduction **1**

1.1 Bryophytes taxonomy 1

1.2 *Physcomitrium patens* leaf development 2

1.3 Mineral Nutrition 4

1.4 Microscopy 5

1.4.1 Light microscopy 5

1.4.2 Fluorescence microscopy 5

1.4.3 Confocal microscopy 6

2 Hypotheses **8**

3 Materials and Methods **9**

3.1 Cultivation of *P. patens* 9

3.2 Cell wall labeling 10

3.3 Microscopy 11

3.3.1 Light/stereo microscopy 11

3.3.2 Confocal microscopy 11

3.3.3 3D Reconstruction 11

3.4 Statistical Analysis 14

4 Results **15**

4.1 Light Microscopy 15

4.2 All measured dimensions were homogeneous among groups. 16

4.3 Comparison between central and border cells variables inside each group. 18

4.3.1 Cells' lengths 18

4.3.2 Cells' widths 20

4.3.3 Cells' wall thickness 21

5 Discussion **23**

5.1 Leaf cell types. 23

5.2 Primary cell wall. 24

5.3 Gametophore formation. 24

6 Conclusions **26**

Literature **27**

List of Figures **37**

7 Supplementary Material **38**

7.1 All measured dimensions were homogeneous among groups. 38

7.2 Comparison between central and border cells variables inside each group. 41

7.2.1 Cells' lengths 41

7.2.2 Cells' widths 44

7.2.3 Cells' wall thickness 47

7.3 Pseudoreplication 50

Chapter 1

Introduction

1.1 Bryophytes taxonomy

From current land plant species, bryophytes are the first group to diverge in the land plant lineage. The bryophytes group is composed of 3 subgroups: mosses, liverworts and hornworts. [7]. Only until very recent it has been resolved that bryophytes comprise a monophyletic group, sister to the tracheophytes. [1, 2, 3, 4, 5, 6]. All display branched filamentous protonemal tissues, and all have a dominant haploid gametophyte generation, in which the sporophyte is dependent on the gametophyte for its development and nourishment [1, 7].

The morphology among the almost 12,000 bryophyte species is quite diverse. In addition to a common protonemal tissue, a leafy or thallus body plan can be expressed on the gametophyte [29]. The first step on the development of the body plan is the germination of an haploid spore, the one will go through a transitory filamentous phase. Depending on how many perpendicular plane divisions are explored by the apical cell, is what will determine the tissue type: protonemal tissue (only one plane), leafy shoots or thalli tissues (two planes), and leafy shoots (three planes) [8, 9].

1.2 *Physcomitrium patens* leaf development

Leaf development in *Physcomitrium patens* starts with the specification of the leaf initial cell, the one keeps a meristematic potential and originates daughter cells (see fig. 1.1), future divisions alternate in the same plane and are almost perpendicular to each other [8, 21]. There is a distinguished morphological difference between young and mature leaves in *P. patens*. The main differences rely on shape changes: 1) of the border cells (longer, narrower and with marginal serrations), and 2) a multicellular midrib. [11, 12].

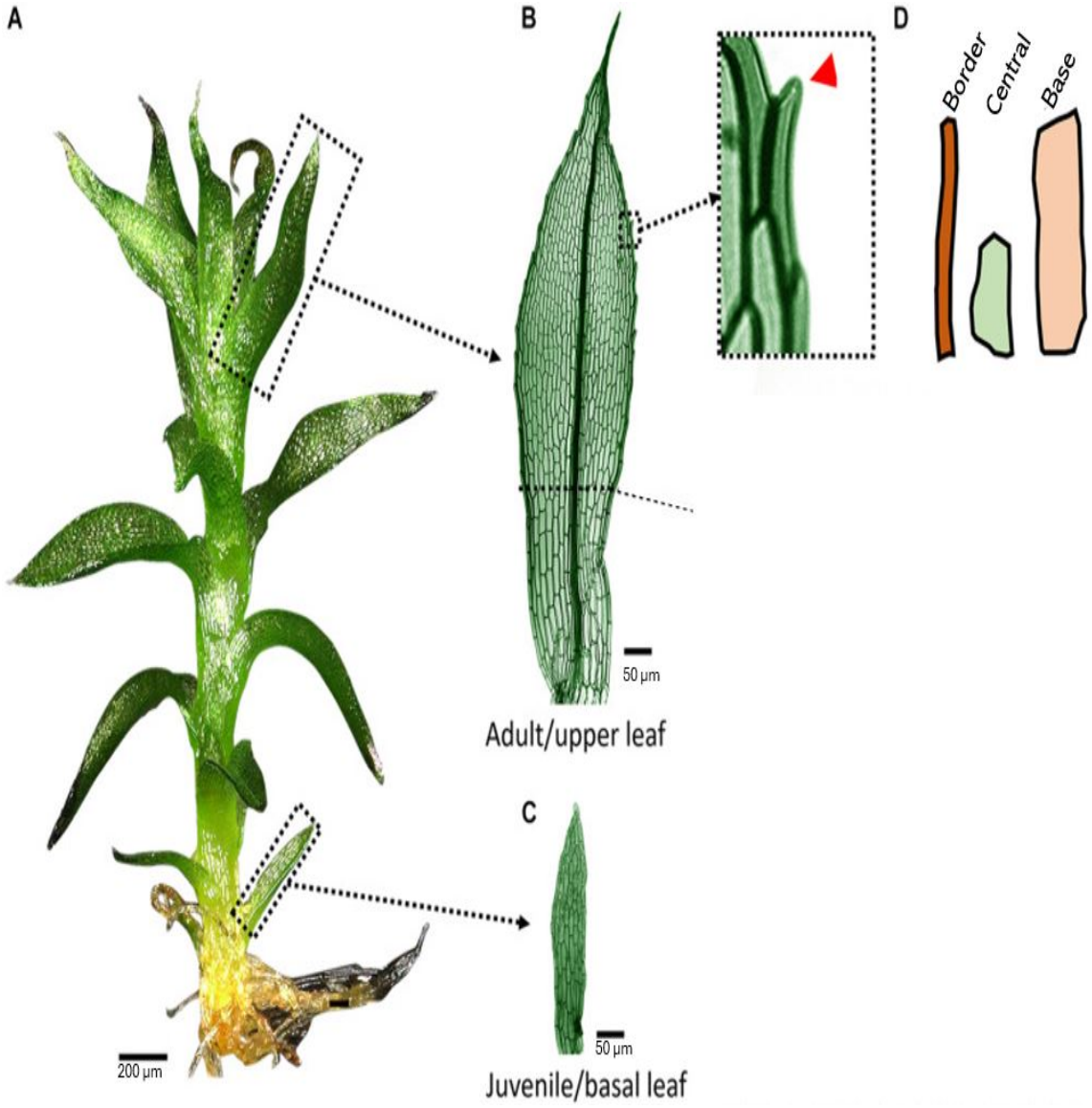

Figure 1.1: Leaf structure in *P. patens*. (A) A shoot. (B) A mature leaf with the border magnified. (C) A young leaf. (D) The 3 cell shapes that can be identified in adult leaves. Figure modified from [21].

1.3 Mineral Nutrition

Only 1.5% of a plant's fresh weight is represented by carbon, hydrogen, oxygen and other atoms. No plant can thrive without water, hence hydrogen and oxygen are essential elements. The same argument holds for nitrogen (e.g. amino acids), phosphorous (e.g. ATP, ribulose 1,5-bisphosphate), sulfur (e.g. cysteine, methionine), magnesium (e.g. chlorophyll) and several additional elements. An element is considered essential if the element is part of a molecule taking part on the structure or metabolism of a plant or/and when the absolute abscence of the element produces aberrations in the plant growth, development or reproduction [16].

Buthe 1860s [16], it was known, that cultured plants would only survive if its solution culture had nitrogen, phosphorus, sulfur, potassium, calcium, magnesium, and iron. By then, carbon was known to be taken up from the air. So, ten elements (including water elements) were recognized as essential elements. With the exception of iron, these elements are needed in relatively large amounts, therefore, they are referred to as macronutrients. The amounts of manganese required were smaller than those of the other elements then known to be essential. Only one element in the classical list of ten (iron) is needed in comparably small amounts (2µmol/g, drymatter). Elements needed in such small amounts are called micronutrients, to distinguish them from the 6 macronutrient elements (N, P, S, K, Ca and Mg). Boron, zinc, copper, molybdenum, chlorine and nickel are also micronutrients [16].

If an atom has a specific density of 5 g/cm^3 or more, it is commonly defined as a heavy metal [17]. As, for example, copper and iron have a density of 8.96 g/cm^3 and 7.87 g/cm^3, respectively, both are at the same time essential micronutrients and heavy metals.

The effects of heavy metals in bryophytes have been reviewed in [18, 29], but

papers reporting specific effects in *P. patens* are very limited. One of these limited reports correspond to [20], where a negative correlation of zinc content to the cell length was found, but not significant correlations of copper content to cell length or cell width were found. However, they reported a trend to form shorter cells in leaves and protonema filaments for copper treated plants.

1.4 Microscopy

1.4.1 Light microscopy

Microscopy is used to increase the optical resolution, which is defined by the distance in which two point-like structures are visible as separated structures. The classic bright field microscope basically consists of a lamp as the light source, a condenser, an objective, and an eye piece. An image of the specimen is projected onto the retina but, following the different lenses, the image is enlarged in the so-called immediate image plane [22]. The theoretically maximal resolution of the light microscope is 0.2 µm according to the equation defined by Abbe: $d = 0.61\ \lambda/A$. In this equation, the resolution (d) depends inversely on the wavelength of the light λ and directly on the numerical aperture of the objective (A) [23].

1.4.2 Fluorescence microscopy

A fluorescence microscope enables the detection of fluorochromes, which emit light with a certain wavelength after excitation by the light of a defined (shorter) wavelength. Generally, arc burner lamps (e.g. mercury arc lamps) are used for illumination as short light wavelengths sources. Nowadays, so-called epifluorescence microscopy is used, where the lamp is placed above the objective and light passes via a specific

filter block through the objective to the specimen. The filter block consists of an excitation filter and a dichromatic mirror (acting as a beam splitter), which illuminate the sample with the light of a defined wavelength, causing the emission of fluorescent light. In addition, the filter block contains an emission filter that allows only the light with an appropriate wavelength to pass through, enabling detection and visualization of the fluorochrome of interest [22].

1.4.3 Confocal microscopy

Another limitation associated with conventional microscopy is its finite depth of focus, which makes it difficult to achieve an image of the object with depth structures. It is therefore impossible to obtain a true 3-D image of a thick object in practice [27]. For a real thick object, by recording a series of sections of the image at different depths (Z-axes) of the object, a complete image of the thick object can be built up in a form of a stack of sections. In other words, a 3-D image of the thick object can be recorded without necessarily slicing the object. A confocal laser scanning microscope contains a fluorescence microscope, different lasers as a light source, a confocal scan head and a computer with an adequate software for acquiring, analyzing and processing the obtained images [27]. The scan head itself consists of a fluorescence filter set, inputs of the external laser light source, a galvanometer-based raster scanning mechanism, different pinhole apertures and some Photonmultipliers (PMTs) [24]. The light beam from the source is directed into the objective lens and then onto a 3-D object. The signal from the illuminated spot is collected by the collection lens and recorded by a point detector. If the thick object is scanned along both axial and transverse directions, a map of the 3-D information, i. e., a 3-D image, may be obtained. To describe 3-D image formation in confocal microscopes, one can use a 3-D point spread function (PSF) which is the image of an ideal point object of the optical system and

then performing a 3D mathematical deconvolution in order to reconstruct the 3D object ([27] and [28]).

Chapter 2

Hypotheses

The main purpose of this study was to discover ultrastructural differences between central and border cells of the leaves of *Physcomitrium patens*, as it has already been reported before that they differ markedly in length and width. Additionally, we wanted to go one step ahead with what was reported before, and go to address the 3D organization of the leaf by staining its cell walls and look under the CLSM in order to have a 3D reconstruction of them. So, based on these ideas, we postulated 2 hypotheses:

I) from all the cell dimensions that we will measure (length, width and cell wall thickness), we expect only cell length to have statistically significant difference between control plants and plants in media enriched with heavy metals (any), as it was the case with zinc [30].

II) we expect only length and width to have statistically significant difference between border and central cells among inside each plant group, as this has been the 2 major morphological differences so far reported between these 2 cell types [21].

Chapter 3

Materials and Methods

3.1 Cultivation of *P. patens*

We propagated *P. patens* specimens as described in [29], at the same time under 4 different conditions. Shortly, by slowly heating on the microwave, the previously prepared media (control medium, media enriched with Fe_3Cl_2, $CuCl_2$, and Fe_3Cl_2 & $CuCl_2$, at 20 µM each one, as this concentration was the maximum when shoot growth happened) was verted into petri dishes of 9 cm diameter inside the laminar flow. Then, after the solidification of the media, 9 samples (bigger than 1 leaf and intended to be of the same size) from a previous control specimen of *P. patens* were planted, with the usage of a forceps, on a 3 x 3 grid on each petri dish. Parafilm was used to seal the petri dishes and they were left for 4 weeks into an incubator (14/10h day/night cycle at 20°C). Control medium as prepared in [29], consists of 1.03 mM $MgSO_4$, 1.86 mM KH_2PO_4, 3.3 mM $Ca(NO_3)_2$, 2.7 mM (NH_4)2-tartrate, 45 µM $FeSO_2$ 9.93 µM, H_3BO_3, 220 nM $CuSO_4$, 1.966 µM $MnCl_2$, 231 nM $CoCl_2$, 191 nM $ZnSO_4$, 169 nM KI, 103 nM Na_2MoO_4, and 0.8% of agar (Sigma Aldrich).

3.2 Cell wall labeling

Even that there exists a standard protocol [31] to use the calcofluor white (CW), from Sigma Aldrich (fluorescent brightener 28, CAT NO. 158067; CAS 4404-43-7), see fig. 3.1), we developed our own protocol. We dropped 5 µL of CW 1% miliQ water on a slide and then place one leaf of the moss in it. We used extremely fine forceps (Roth 1P2X) to pull single and mature (those lying at the top of the gametophyte) leaves from its base. After taking out the slide with the samples already lying on them, from the chamber flow, we added between 3-5 CW 1% µL, until the leaf is completely immersed in the drop. The goal is to have the leaf completely immersed for 45 minutes avoiding the evaporation of the drop, in total 3 to 4 more drops of 3-5 CW 1% µL (each one) needed to be added every 10-15 minutes. Once the 45 minutes have passed, let the drop to evaporate and now add miliQ water to moist it enough to prepare it for laying over the cover glass.

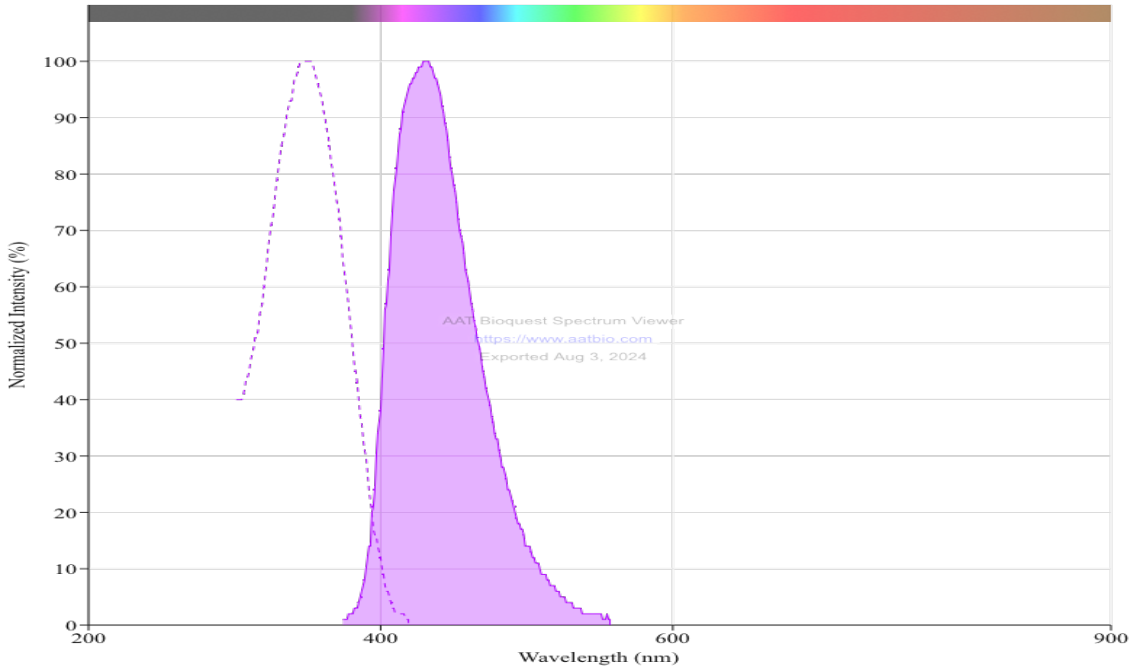

Figure 3.1: The absorption (maximum at 350nm) and emission (maximum at 432nm) spectrum of "Calcofluor White 2MR Sigma-Aldrich". Figure taken from [13].

3.3 Microscopy

3.3.1 Light/stereo microscopy

First, we observed *P. patens* under the stereo microscope zeiss stemi 355 [32]. We saw different petri dishes (without opening them) corresponding to 3 different growing media conditions: control, media enriched with Fe_3Cl_2 and $CuCl_2$, at 20µM, respectively.

3.3.2 Confocal microscopy

At least 2 leaves from specimens of *P. patens* under each of 4 different conditions: control medium, media enriched with Fe_3Cl_2, $CuCl_2$, and Fe_3Cl_2 & $CuCl_2$, at 20 µM each one, were analyzed under the Confocal Laser Scanning Microscope (CLSM) Leica microscope TCS SP8 DM-600 to get fluorescence images of the cell walls, then image stacks to make 3D reconstructions from them.

LAS X [33] is the incorporated software of the CLSM Leica microscope TCS SP8 DM-600, the one allows remote manipulation of the microscope and acquisition and collection of the images taken by the microscope camera. Inside this software is where the settings for the images acquisition were established: 1) only one laser was needed, the 405nm diode one, with a power of 30.2%, 2) only one PMT tube was needed, with a detection interval between 415-465nm.

3.3.3 3D Reconstruction

Also, inside the LAS X software, the settings for the Z-stacks were established: 1) pixel format: 256x256, 2) Speed of scanning: 200, 3) Line Accuracy: 3, 4) Frame

Accuracy: 2, 5) Line Average: 1, and 6) Frame Average: 1. On several cases, it was not possible to keep a constant number of steps (35) and Z-step size (0.87nm), but on those cases one of them was fixed, the one that required the less amount of time. After acquiring all the Z-stack pictures, by clicking the 3D embedded window of the LAS X software is where the 3D reconstruction was visible. Also, in this 3D feature of the software is where the measurement of distances is possible and were the 3 different types of measurements were performed (cell length, width and cell wall thickness), see figs. 3.2 and 3.3.

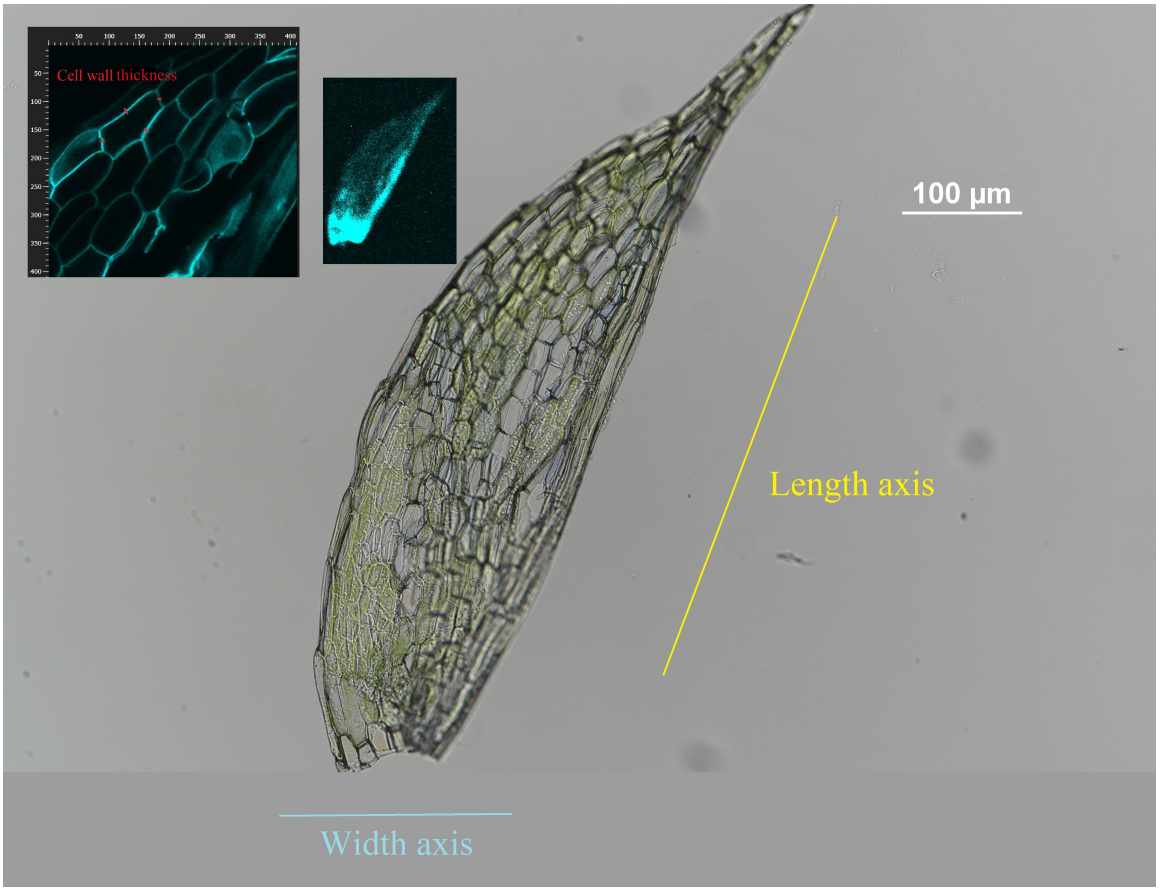

Figure 3.2: Determination of length, width and cell wall thickness axes.

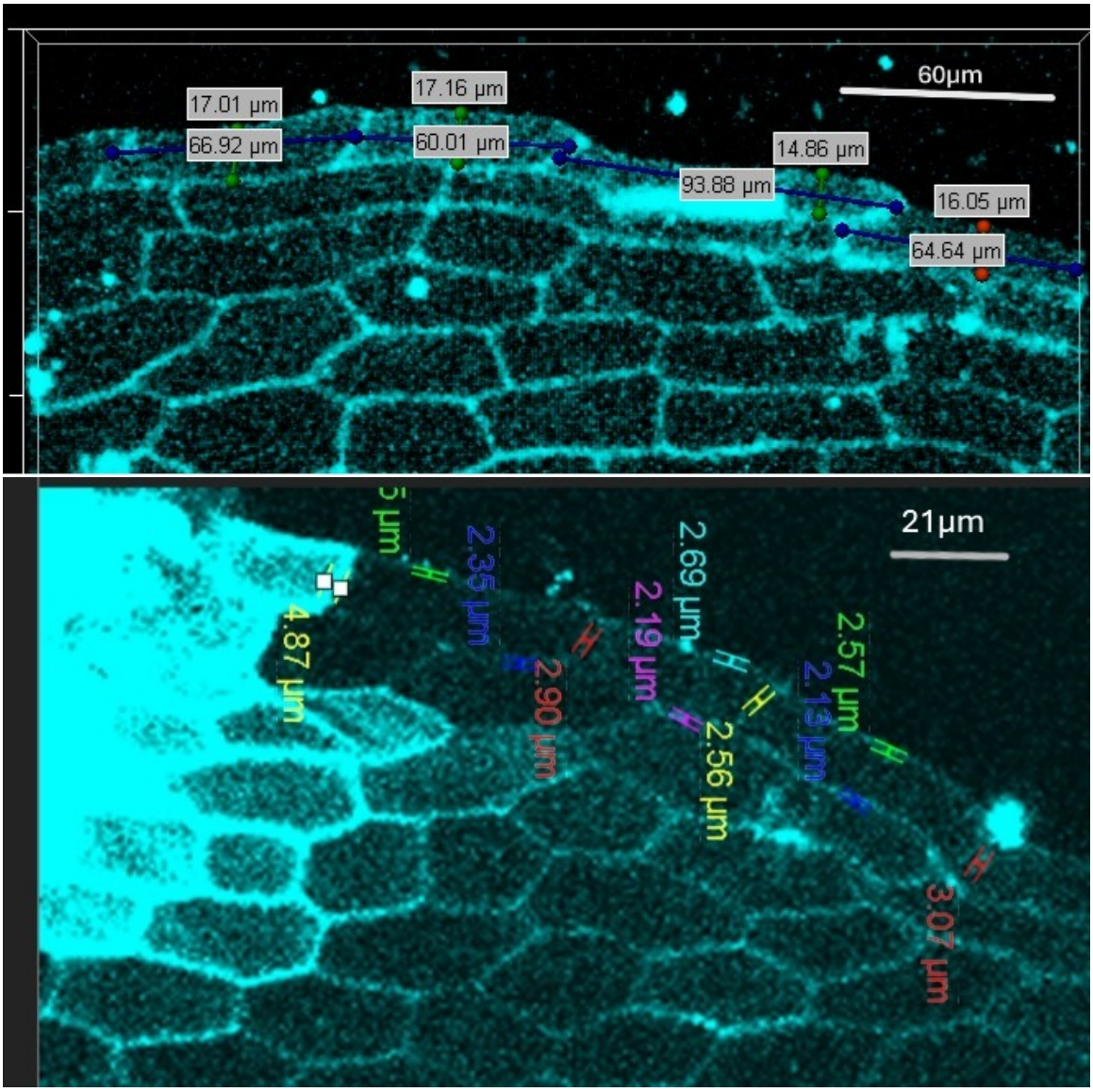

Figure 3.3: Measure examples. Length and width (top) and cell wall thickness (bottom).

3.4 Statistical Analysis

The majority of the statistical analyses were performed with Statigraphics 19 centurion software [34]. The rest were performed with SPSS v.31 [35] (normality tests and some Levene´s tests). We performed normality tests, Levene´s tests, one-way ANOVA tests, t-tests and box-whisker plots (see [42]). To test the first hypothesis: from all the cell dimensions that we measured (length, width and cell wall thickness), we expect only cell length to have statistically significant difference between plants of *P. patens* grown in control medium and plants grown in media enriched with heavy metals (any), we used all the mentioned tests (except for t-tests) for each 1 of the 3 variables measured (length, width and cell wall thickness). For the second hypothesis: from the cell dimensions that were measured, we expect length and width to have statistically significant difference between border and central cells among inside each group. To test this, we only needed to use t-tests (and 2 ANOVA tests, for those cases without homogeneous variances) between border and central measures inside each one of the 4 plant groups.

Chapter 4

Results

4.1 Light Microscopy

Under the stereoscope we were able to appreciate the anatomy and morphology of *P. patens* leaves. Also, we were able to appreciate, the morphological stress (bleaching) caused by being cultivated with heavy metal components (figure 4.1).

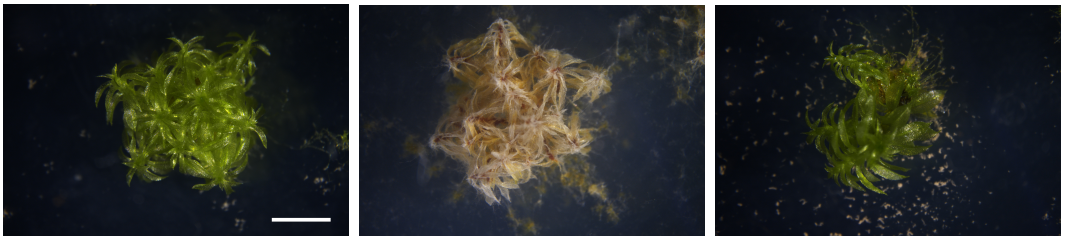

Figure 4.1: Observations under the stereoscope for plants grown under control (left), copper (center) and iron (right) conditions. Same scale bar (2 mm) applies to all.

4.2 All measured dimensions were homogeneous among groups.

We did not find significant differences ($p < 0.05$) between the groups (fig. 4.2) on each variable measured (length, width and cell wall thickness). Normality tests, variance homogeneity tests, p-value tables, summary statistics and whisker-box plots can be found in the supplementary material section 7.1.

We first used a 1 way ANOVA test over all the measured cells inside a leaf, and by following this model we got the first graphs (see figs. 7.18 and 7.19). But then we realized that this approach would be a pseudoreplication statistical model [41], as we saw that the variance between cells of different leaves of the control group (between subjects) was significant and greater than the variance inside the cells of the same leaf (between subjects). This made us think that we would have gotten false positives with the first statistical approach, so we changed to a second statistical model, were we also used a 1 way ANOVA test, but this time by only using 1 central and 1 border cell measures per each leaf, being able to have data of 5 leaves per condition. With this second statistical model we were able to confirm our guess, that the first graphs were false positives (showing significant differences) for all the variables, as the graphs of the second model did not show any significant difference. As there was not significant difference for any of the variables, we can say that the first hypothesis did not stand, but at the same time we can not reject it yet, as a higher amount of leaves would be needed to be measured to reach a statistical power of 80% (see fig. 4.2) [42]. Additionally, since no significant difference was retrieved, we cannot address the specific effects on the plant physiology of the factors (grown conditions).

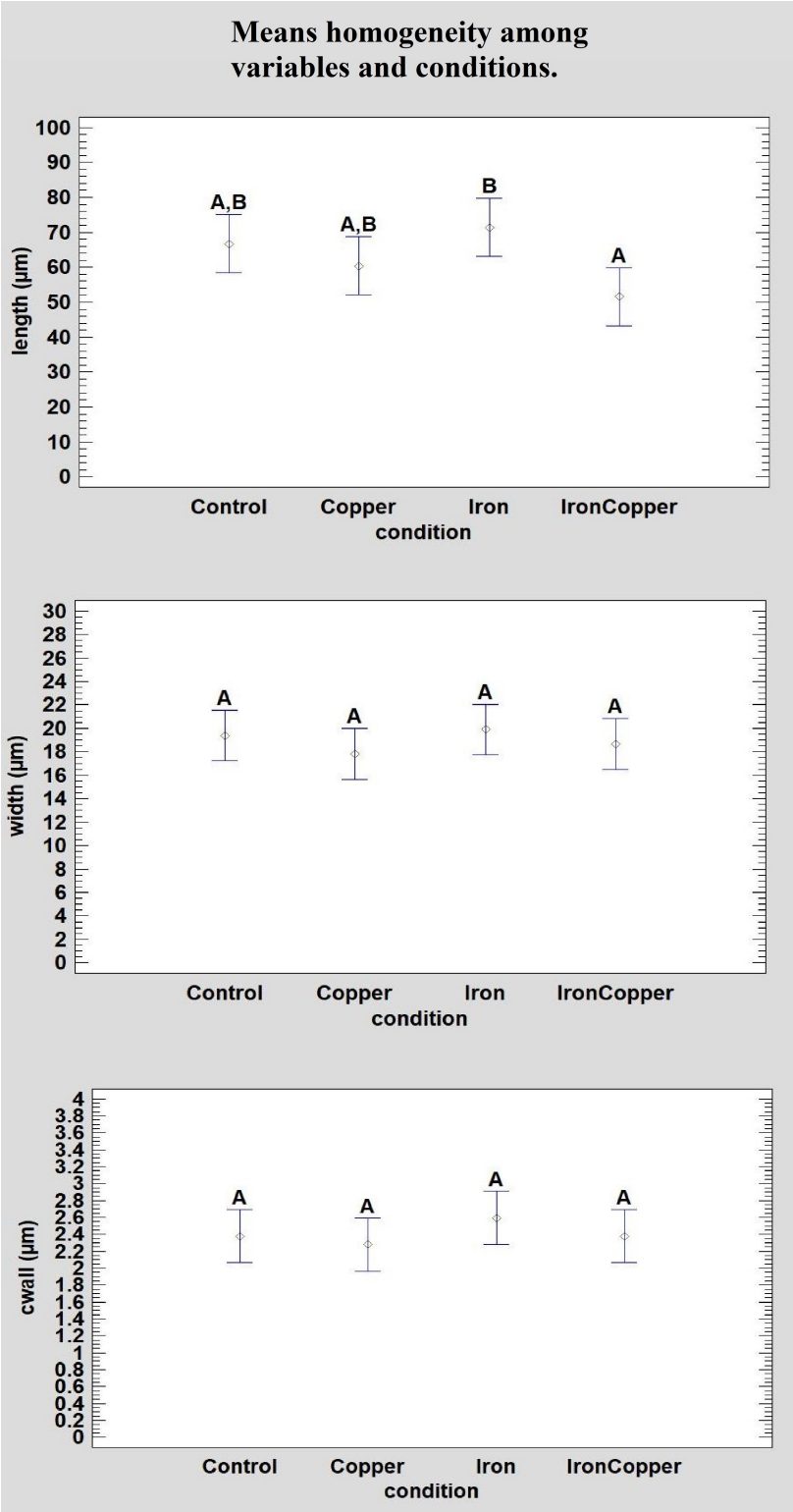

Figure 4.2: Means plots performed for each measured variable among the different conditions. Length (top), width (middle) and cell wall thickness (bottom). The statistical power was 0.491, 0.113 and 0.111, and the amount of leaves needed to be sampled to reach a statistical power of 0.8 was 36, 188 and 192, respectively.

4.3 Comparison between central and border cells variables inside each group.

4.3.1 Cells' lengths

We found significant difference ($p < 0.05$), between central cells and border cells lengths for 3 of the 4 groups (being the exception the ironcopper condition, see fig. 4.3). Being the border cells longer than central cells. For all the variables, normality tests, variance homogeneity tests, p-value tables and summary statistics of each group can be found in the supplementary material in section 7.2.

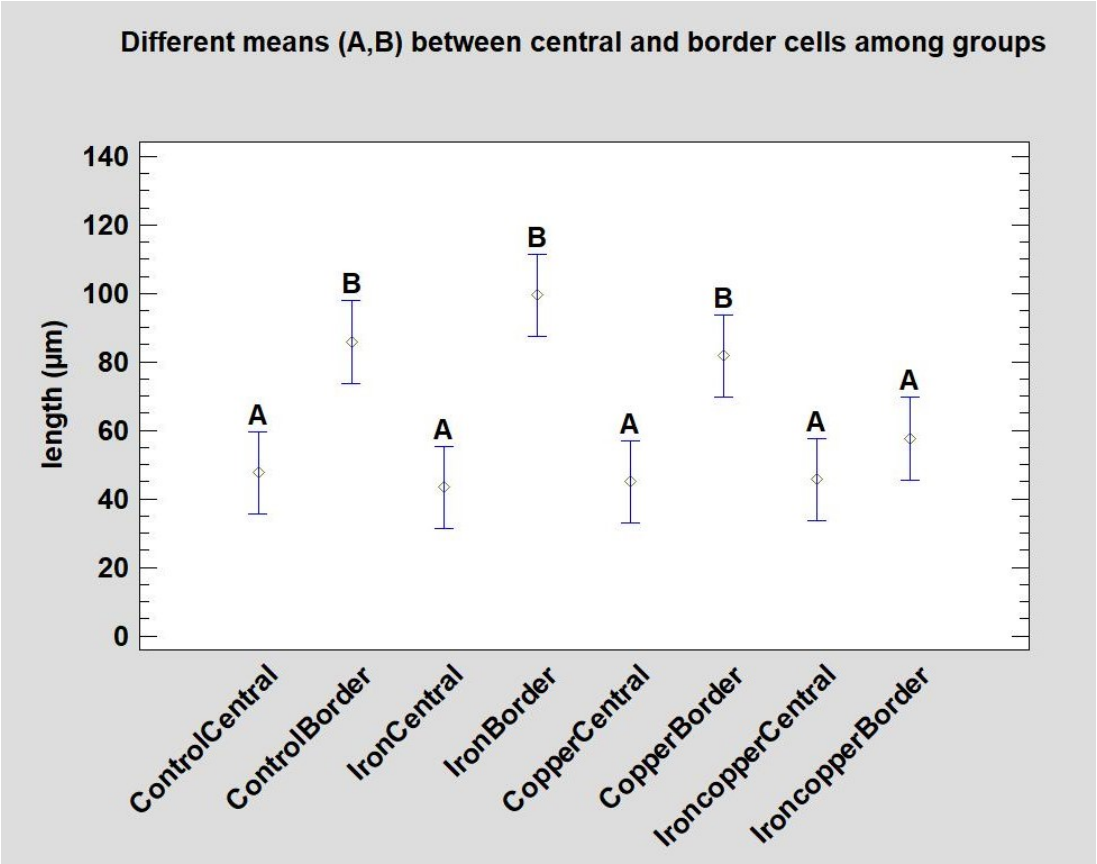

Figure 4.3: Central and border cells means plot for the 4 conditions. For ironcopper the statistical power obtained was 0.308 and the amount of leaves needed to be sampled to reach a statistical power of 0.8 was 30.

Our second hypothesis did not stand as the ironcopper group did not show significant difference between central and border cells. But this is not definitive, as we only reach a statistical power of 30%, and in order to reject it with a higher confidence interval, we would need to reach at least a 80% one [42].

4.3.2 Cells' widths

We found significant difference ($p < 0.05$), between central cells and border cells widths for 2 groups (being the exception the control and ironcopper conditions, see fig. 4.4). Being the border cells narrower than central cells.

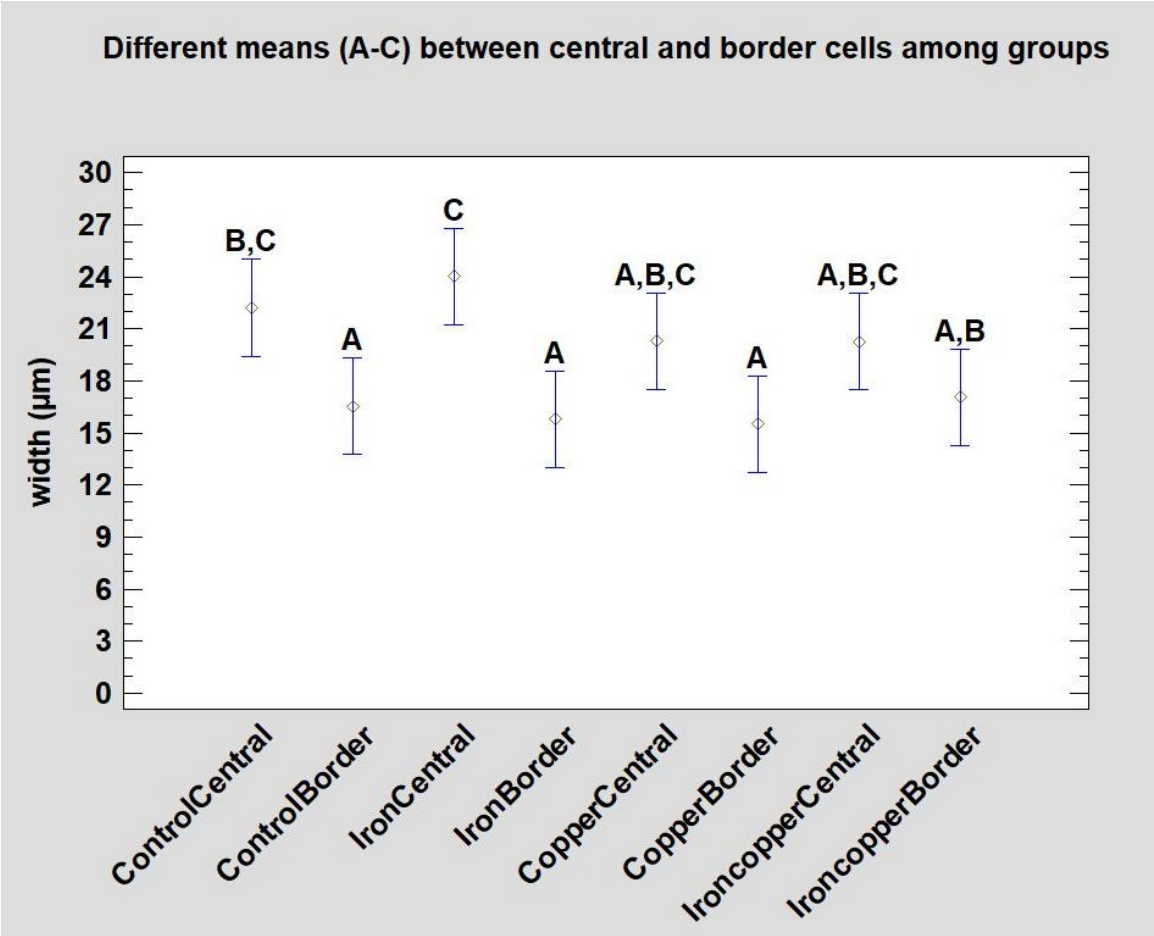

Figure 4.4: Central and border cells means plot for the 4 conditions. For the control and ironcopper groups, the statistical power obtained was 0.2501 and 0.2308, and the amount of leaves needed to be sampled to reach a statistical power of 0.8 was 36 and 44, respectively.

The expected difference (false positive) between the first and second statistical approach only happened in the control group (see fig. 7.19). The second hypothesis also did not stand, as 2 groups (control and ironcopper) did not show significant difference between central and border cells. But this is not definitive, as we only

reached a statistical power of 24%, average between both, and in order to reject it with a higher confidence interval, we would need to reach at least a 80% one [42].

4.3.3 Cells' wall thickness

We only found a significant difference ($p < 0.05$), between central cells and border cells´ walls thickness in the ironcopper group (fig. 4.5), with the border cells´ walls thicker than the central cell ones.

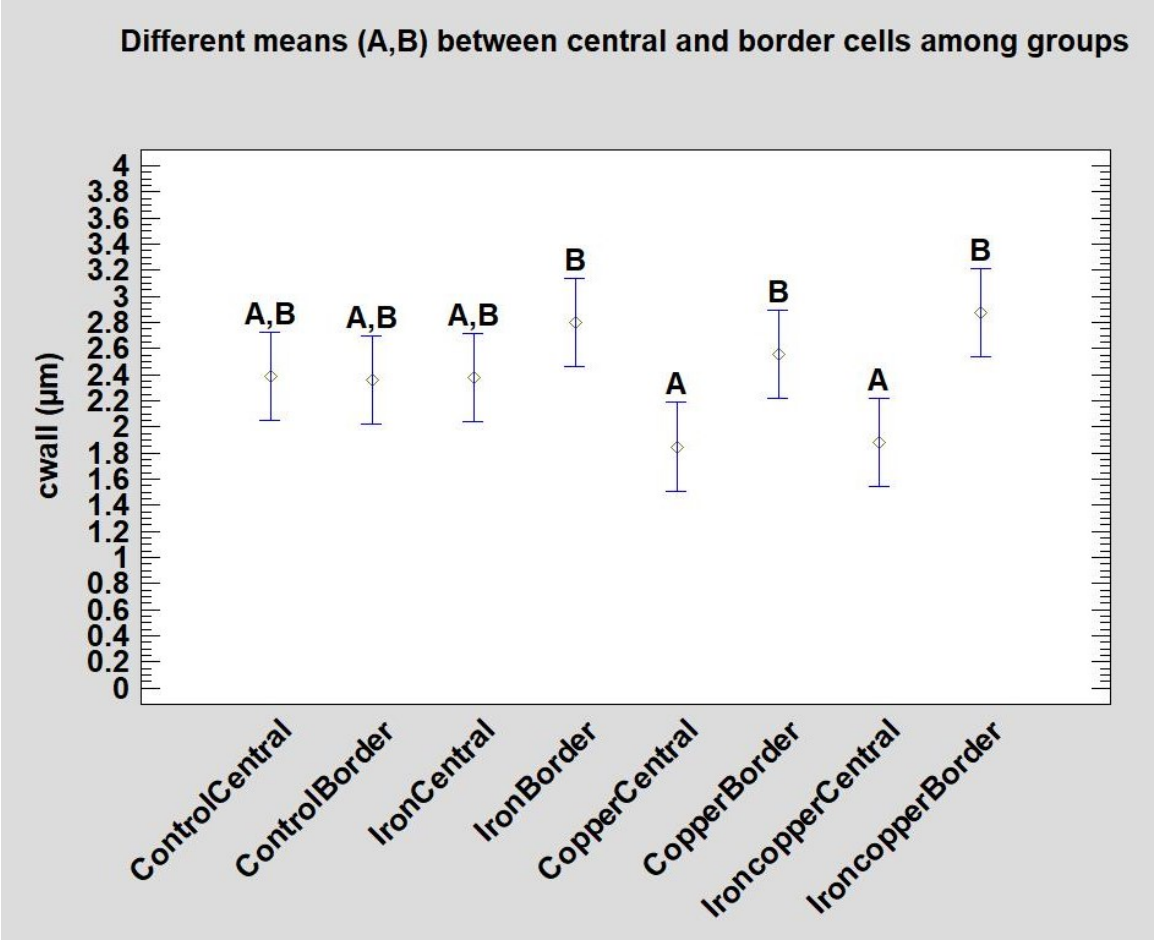

Figure 4.5: Central and border cells means plot for all the 4 groups. For the control, iron and copper groups, the statistical power obtained was 0.0286, 0.2965 and 0.4182, and the amount of leaves needed to be sampled to reach a statistical power of 0.8 was 17966, 32, 22, respectively.

For the cell wall thickness variable, the expected difference (false positive) between

the first and second statistical approach happened in 2 groups (control and iron, see fig. 7.19). It is for this variable, the reason why we can deny for complete our second hypothesis, as we found a significant difference for a variable different of length and width. This finding tells us that there are more morphological differences, in addition to the reported in the literature (length and width), to be unrevealed between the 2 cell types [43].

Chapter 5

Discussion

5.1 Leaf cell types.

As it happens with *Sphagnum spp.* [44], that at least 2 different cell types exist on its leaves for 2 different physiological roles (photosynthesis and water conductance), one question that we wanted to address with this study was: if different cell-type traits change due to stress conditions. Specifically in this study, if the anatomical traits of border and central cells would be affected by heavy metal stress. In principle, following the idea that cell-types are high dimensional attractors [43], we would not expect things like dedifferentiations or cell-fate changes to occur. And is because of this reason why we would have expected that the anatomical traits measured here between the 2 cell-types remain constant among all the groups, but that was not the case, raising the question if we are under a slight cell-type change scenario caused by heavy metal stress.

5.2 Primary cell wall.

Recently, in bryophytes, it was shown that there is almost no correlation between cell wall thickness and leaf size [45], and ultimately that cell wall thickness is not a structural unit giving support to the rigidity and strength of the leaves. This implies that the function of cell walls are basic ones: as water conductance (apoplast) and storage. If we assume that cell wall composition and/or anatomy (dimension) are flexible, changes on them can be addressed to specific requirements of the cells due to internal or external changes. The veracity of the last statement is still in debate, as in this study, we did not find an anatomical difference between the cell walls of *P. patens* individuals under heavy metal stress and the control, to check composition will be a future task.

5.3 Gametophore formation.

Another interesting thing was the discovery of a copper tolerance threshold for the formation of gametophores. We were only able to recover gametophores by lowering the concentration of copper to 20 µM or lower. We wonder if this limitation is caused by physiological (photosynthesis), developmental (gametophore apical cells) or both malfunctions. If it is physiological, copper atoms are essential part of the plastocyanin protein, which is part of the electron transfer chain of the phosphorylation part of the photosynthesis [46]. Under copper (Cu^{2+})stress: "the proportion of open photosystem two (PSII) reaction centers is dramatically decreased and the first quinone acceptor reoxidation is fully inhibited" [Padua2010], reducing the efficiency of the photophosphorylation and ultimately the production of adenosyntriphosphate (ATP). However, if the negative impact is on a developmental program, it would be interesting to find out which of the 2 main pathways that promote the formation of

gametophore apical cells (auxin or cytokinin-mediated) are disrupted by the copper atoms ([48] and [49]).

Chapter 6

Conclusions

The sample size was not enough to distinguish factor effects (grown conditions) on the dependent variables (length, width and cell wall thickness). However, a tendency of differences already can be seen. The growth conditions affect the natural morphological differences between border and central cells for all the variables. Finally, as it was shown for cell wall thickness, more morphological differences between border and central cell types remain to be discovered (e.g. cell height).

Bibliography

[1] Dong S., Wang, S., Li, L. et al.; "Bryophytes hold a larger gene family space than vascular plants". *Nature Genetics, vol. 57, pp. 2562-2569, 2025.*

[2] Leebens-Mack J., Barker M., Carpenter E., Deyholos M., et al.; "One thousand plant transcriptomes and the phylogenomics of green plants". *Nature, vol. 574, pp. 679-685, 2019.*

[3] Su D., Yang L., Shi X., Ma M., Zhou X., Hedges B. and Zhong B.; "Large-scale phylogenomic analyses reveal the monophyly of bryophytes and neoproterozoic origin of land plants". *Mol. Biol., vol. 38, pp. 3332-3344, 2021.*

[4] Harris B., Clark J., Schrempf D., Szöllősi D., Donoghue P., Hetherington A. and Williams T.; "Divergent evolutionary trajectories of bryophytes and tracheophytes from a complex common ancestor of land plants". *Nat Ecol. Evol., vol. 6, pp. 1634-1643, 2022.*

[5] Harris B., Harrison J., Hetherington A. and Williams T.; "Phylogenomic evidence for the monophyly of bryophytes and the reductive evolution of stomata". *Curr. Biol., vol. 30, pp. 2001-2012, 2020.*

[6] de Sousa F., Foster P., Donoghue P., Schneider H. and Cox C.; "Nuclear protein phylogenies support the monophyly of the three bryophyte groups (Bryophyta Schimp.)". *New Phytol., vol. 222, pp. 565-575, 2019.*

[7] Hirt H.;"Plant Stress Biology". *Wiley-Blackwell* 2009, pp 17-19.

[8] Harrison J., Roeder A., Meyerowitz E. and Langdale J.; "Local Cues and Asymmetric Cell Divisions Underpin Body Plan Transitions in the Moss Physcomitrella patens". *Cell Press, vol. 19, No. 6, pp. 461-471, 2009.*

[9] Schumaker K. and Dietrich M.; "Programmed changes in form during moss development". *Plant Cell, vol. 9, pp. 1099-1107, 1997.*

[10] Bascom, C., Wu S., Nelson K., Oakey J. and Bezanilla M.; "Long-Term Growth of Moss in Microfluidic Devices Enables Subcellular Studies in Development". *Plant Physiology, vol. 172, No. 1, pp. 28-37, 2021.*

[11] Barker E. and Ashton N.; "Heteroblasty in the moss, *Aphanoregma patens (Physcomitrella patens)*, results from progressive modulation of a single fundamental leaf developmental program". *J. Bryol., vol. 35, pp. 185-196, 2013.*

[12] Dennis, R., Whitewoods C. and Harrison J.; "Quantitative methods in like-for-like comparative analyses of *Aphanoregma patens (Physcomitrella patens)* phyllid development". *Journal of Bryology, vol. 41, No. 4, pp. 314-321, 2021.*

[13] `https://www.aatbio.com/fluorescence-excitation-emission-spectrum-graph-viewer/calcofluor_white_2mr` accessed 18th of april 2026.

[14] Petschinger K., Adlassnig W., Sabovljevic M. and Lang I.; "Lamina cell shape and cell wall thickness are useful indicators for metal tolerance - an example in bryophytes". *Plants, vol. 10, pp. 274.284, 2021.*

[15] Donner T., Sherr I., Scarpella E.; "Regulation of preprocambrial cell state acquisition by auxin signaling in *Arabidopsis* leaves". *Development, vol. 136, pp. 3235-3246, 2009.*

[16] Epstein E. and Bloom. A.;"Mineral nutrition of plants: Principles and perspectives". *Sinauer Associates, Inc.* 2002, pp14, 46, 50.

[17] Järup L.; "Hazards of heavy metal contamination". *British Medical Bulletin, vol. 68, pp. 167-182, 2003.*

[18] Stankovic J., Sabovljevic A. and Sabovljevic M.; "Bryophytes and heavy metals: a review". *Acta Bot. Croat, vol. 77, no. 2 pp. , 2018.*

[19] Rother M., Krauss G., Grass G., and Wesenberg D.; "Sulphate assimilation under Cd2+ stress in *Physcomitrium patens*- combined transcriptomics, enzyme and metabolite profiling". *Plant, Cell and Environment, vol. 29, pp. 1801-1811 , 2006.*

[20] Sassman S., Weidinger M., Adlassnig W., Hofhansl F., Bock B. and Lang I.; "Zinc and copper uptake in *Physcomitrella patens*: limitations and effects on growth and morphology". *Environmental and experimental botany, vol. 118, pp. 12-20, 2015.*

[21] Lin W., Wang Y., Coudert Y.and Kierzkowski D.; "Leaf morphogenesis: insights from the moss *Physcomitrium patens*". *Frontiers in plant science, vol. 12, pp. 167-185, 2021.*

[22] Krauss G-J and Nies D.H.; "Ecological biochemistry. environmental and interspecies interactions". *Wiley-VCH, 1st edition, pp. 367, 370 2015.*

[23] Kohler H.; "On Abbe's theory of image formation in the microscope". *Optica acta: international journal of optics, vol. 28:12, pp. 1691-1701, 1981.*

[24] Douglas B.; "Confocal laser scanning microscopy". *https://doi-org.uaccess.univie.ac.at/10.1002/9781118382905.ch13* ***1****, (2024).*

[25] Paddock, S.W.; "Principles and practices of laser scanning confocal microscopy". *Molecular Biotechnology,* ***16****, 3, (2000), pp. 127-149.*

[26] Sheppard C. and Choudhury A.; "Image formation in the scanning microscope". *Optica Acta, vol. 24 (1977), pp.1051-1073.*

[27] Gu M.; "Principles of Three-Dimensional Imaging in Confocal Microscopes". *Wspc, (1996), pp. 1-3, 5.*

[28] Yoo S., Ruiz P, Huang X., He K., Ferrier N., Hereld M., Selewa A., Daddysman M., Scherer N., Cossairt O. and Katsaggelos A.; "3d image reconstruction from multi-focus microscope: axial super-resolution and multiple-frame processing". *EEE International Conference on Acoustics, Speech and Signal Processing (ICASSP), Calgary, AB, Canada, 2018, pp. 1453-1457*

[29] Schillaci L., Nevena D. and Lang I.; "Is a combination of metals more toxic to mosses than a single metal". *Plants, vol. 12, no. 3960, pp. 1-14, 2023.*

[30] Lang I. and Wernitznig S.; "Sequestration at the cell wall and plasma membrane facilitates zinc tolerance in the moss *pholia drumondii*". *Environmental and experimental botany, vol. 74, pp. 186-193, 2011.*

[31] Kurihara D., Mizuta Y., Sato Y. and Higashiyama T.; "ClearSee: a rapid optical clearing reagent for whole-plant fluorescence imaging". *Development, vol. 142, pp. 4168-4179, 2015.*

[32] `https://www.zeiss.com/microscopy/en/c/edr/26/zeiss-stemi-355-stereo-microscope.html?utm_source=google&utm_medium=search-ad&utm_campaign=mc_16322_cv_edr_apem_Feb26_stemi-355-Brand&utm_adgroup=%7badgroupid%7d&utm_term=%7bkeyword%7d&gad_source=1&gad_campaignid=23595589133&gbraid=0AAAAA-O5Kf7-mEqqERgT4tbYd2awK4StN&gclid=`

Cj0KCQjw-pHPBhCdARIsAHXYWP_olhpkH36B-ApVxU-8ywuokW10uy2NaC7c0MfpI8wfes14U99rIx
wcB, accessed 18th of april 2026.

[33] https://www.leica-microsystems.com/products/microscope-software/p/leica-las-x-ls/?country=MX, accessed 18th of april 2026.

[34] https://www.statgraphics.com/centurion-19, accessed 18th of april 2026.

[35] https://www.ibm.com/support/pages/node/7256141#en, accessed 18th of april 2026.

[36] Konno H., Nakashima S. and Katoh K.; "Metal-tolerant moss *Scopephila cataractae* accumulates copper in the call wall pectin of the protonemata". *Plants, vol. 167, pp. 358-364, 2010.*

[37] Krzeslowska M., Lenartowska M., Mellerowicz E., Samardakiewicz S. and Woźny A.; "Pectinous cell wall thickenings formation-A response of moss protonemata cells to lead". *Environmental and experimental Botany, vol. 65, pp. 119-131, 2009.*

[38] Panda S. and Choudhury S.; "Changes in nitrate reductase activity and oxidative stress response in the moss *Polythricum commune* subjected to chromium, copper and zinc phytotoxicity". *J. Plant Physiology, vol. 17, no. 2, pp. 191-197, 2005.*

[39] Basile A., Sorbo S., Pisani T., Paoli L., Munzi S. and Loppi S.; "Bioaccumulation and ultrastructural effects of Cd, Cu, Pb and Zn in the moss *Scorpiurum circinatum* (Brid.) Fleisch & Looske". *Environmental pollution, vol. 166, pp. 208-211, 2012.*

[40] Tremper A., Agneta M., Burton S. and Higgs D.; "Field and laboratory exposure of two moss species to low level metal pollution". *Journal of atmospheric chemistry, vol. 49, pp. 11-120, 2004.*

[41] Doncaster P.; "Analysis of Variance and Covariance How to Choose and Construct Models for the Life Sciences". *Cambridge University Press & Assessment, pp. 62, 2009.*

[42] Martinez-Gonzalez M., Sanchez-Villegas A. and Faulin J.; "Bioestadistica amigable". *Ediciones Diaz de santos, 2006.*

[43] Huang S., Eichler G., Bar-Yam Y. and Ingber D.; "Cell Fates as High-Dimensional Attractor States of a Complex Gene Regulatory Network". *Physical review letters, vol. 94, no. 128701, pp 1-4, 2005.*

[44] Ningjing L., Qiuqi G., Fangming S., Lei G., Yongqi L., Yiwen W., Zhiwei G., Haoran L., Yue S., Bosheng L., Bing N., Rui-Liang Z. and Qiong Z.; "Developmentally controlled subcellular remodeling and VND-initiated vacuole executed PCD module shape xylem-like cells in peat moss". *communications biology, vol. 7, no. 1323, pp 112, 2024.*

[45] Mir-Rossello P. M., Flexas J. and Carriqui M.; "Leaf size in mosses is structurally constrained by cell dimensions and genome size". *plant biology, vol. 28, pp. 420–431, 2025.*

[46] Hall D. O. and Rao K. K.; "Photosynthesis". *Cambridge university press, fifth edition, pp 79-86, 1994.*

[47] Padua M., Cavaco A. M., Aubert S., Bligny R. and Casimiro A.; "Effects of copper on the photosynthesis of intact chloroplasts: interaction with manganese". *Physiologia plantarum, vol. 138, pp. 301-311, 2010.*

[48] Aoyama T., Hiwatashi Y., Shigyo M., Kofuji R., Kubo M., Ito M. and Hasebe M.; "AP2-type transcription factors determine stem cell identity in the moss Physcomitrella patens". *Development, vol. 139, no. 17, pp 3120-3129, 2012.*

[49] Hata Y., Ohtsuka J., Hiwatashi Y., Naramoto S. and Kyozuka J.; "Cytokinin and ALOG proteins regulate pluripotent stem cell identity in the moss Physcomitrium patens". *Science advances, vol. 10, no. 35, pp 1-12, 2024.*

List of Figures

1.1 Leaf structure in *P. patens*. (A) A shoot. (B) A mature leaf with the border magnified. (C) A young leaf. (D) The 3 cell shapes that can be identified in adult leaves. Figure modified from [21]. 3

3.1 The absorption (maximum at 350nm) and emission (maximum at 432nm) spectrum of "Calcofluor White 2MR Sigma-Aldrich". Figure taken from [13]. 10

3.2 Determination of length, width and cell wall thickness axes. 12

3.3 Measure examples. Length and width (top) and cell wall thickness (bottom). 13

4.1 Observations under the stereoscope for plants grown under control (left), copper (center) and iron (right) conditions. Same scale bar (2 mm) applies to all. 15

4.2 Means plots performed for each measured variable among the different conditions. Length (top), width (middle) and cell wall thickness (bottom). The statistical power was 0.491, 0.113 and 0.111, and the amount of leaves needed to be sampled to reach a statistical power of 0.8 was 36, 188 and 192, respectively. 17

4.3 Central and border cells means plot for the 4 conditions. For ironcopper the statistical power obtained was 0.308 and the amount of leaves needed to be sampled to reach a statistical power of 0.8 was 30. . . . 18

4.4 Central and border cells means plot for the 4 conditions. For the control and ironcopper groups, the statistical power obtained was 0.2501 and 0.2308, and the amount of leaves needed to be sampled to reach a statistical power of 0.8 was 36 and 44, respectively. 20

4.5 Central and border cells means plot for all the 4 groups. For the control, iron and copper groups, the statistical power obtained was 0.0286, 0.2965 and 0.4182, and the amount of leaves needed to be sampled to reach a statistical power of 0.8 was 17966, 32, 22, respectively. 21

7.1 Normality tests (Shapiro-Wilkins and Kolmogorov-Smirnof) performed over the residuals of length (lengthRes), width (widthRes) and cell wall thickness (cwallRes) variables distributed normally ($P > 0.05$). 39

7.2 Levene's tests (homogeneity of variances) performed over the residuals of length (top left), width (top right) and cell wall thickness (bottom left) variables showed homogeneity of the variances ($P > 0.05$). 39

7.3 p-values of ANOVA tests. Length (top left), width (top right) and cell wall thickness (bottom left). 39

7.4 Summary statistics of each measured variable among the different conditions. Length (top left), width (top right) and cell wall thickness (bottom left). 40

7.5 Box-whisker plots performed for each measured variable among the different conditions. Length (top left), width (top right), and cell wall thickness (bottom left). 40

7.6 Normality tests (Shapiro-Wilkins and Kolmogorov-Smirnof) performed over the length measures of the 4 conditions (control, iron, copper and ironcopper), distributed normally ($P > 0.05$). 42

7.7 Levene's tests (homogeneity of variances) performed over length measures of the 4 conditions (control, iron, copper and ironcopper). Only the iron and copper groups did not have homogeneous variances ($P < 0.05$). 43

7.8 p-values of t (top left and bottom right) and ANOVA tests (top right and bottom left) over length measures. Control (top left), iron (top right), copper (bottom left) and ironcopper (bottom right). 43

7.9 Summary statistics of length measures. Control (top left), iron (top right), copper (bottom left) and ironcopper (bottom right). 44

7.10 Normality tests (Shapiro-Wilkins and Kolmogorov-Smirnof) performed over the width measures of the 4 conditions (control, iron, copper and ironcopper), distributed normally ($P > 0.05$). 45

7.11 Levene's tests (homogeneity of variances) performed over width measures of the 4 conditions (control, iron, copper and ironcopper) showed homogeneous variances ($P > 0.05$) between border and central cells. . 46

7.12 p-values of t tests over width measures. Control (top left), iron (top right), copper (bottom left) and ironcopper (bottom right). 46

7.13 Summary statistics of width measures. Control (top left), iron (top right), copper (bottom left) and ironcopper (bottom right). 47

7.14 Normality tests (Shapiro-Wilkins and Kolmogorov-Smirnof) performed over the cell wall thickness measures of the 4 conditions (control, iron, copper and ironcopper), distributed normally ($P > 0.05$). 48

7.15 Levene's tests (homogeneity of variances) performed over cell wall thickness measures of the 4 conditions (control, iron, copper and ironcopper) showed homogeneous variances ($P > 0.05$) between central and border cells. 49

7.16 p-values of t tests over cell wall thickness measures. Control (top left), iron (top right), copper (bottom left) and ironcopper (bottom right) between central and border cells. 49

7.17 Summary statistics of cell wall thickness measures. Control (top left), iron (top right), copper (bottom left) and ironcopper (bottom right). 50

7.18 Mean plots of the ANOVA tests for the first statistical model (with pseudoreplication). Length (top), width (central) and cell wall thickness (bottom). 51

7.19 Means plots of the ANOVAs tests, of the first statistical model (with pseudoreplication) between central and border cells for the first statistical model for the three variables. Length (top), width (central) and cell wall thickness (bottom). 52

Chapter 7

Supplementary Material

On the following pages the supplementary graphs of results sections 4.2 and 4.3 are reported. Also, the main graphs obtained with the first statistical model are given (pseudoreplication).

7.1 All measured dimensions were homogeneous among groups.

Here we show that the residuals of each one of the 3 variables followed a normal distribution (fig. 7.1). They also showed homogeneous variances (fig. 7.2). Due to these 2 things, only parametric tests were performed subsequently. Here we also report the ANOVA p-values (fig. 7.3), summary statistics (fig. 7.4) and whisker-box plots (fig. 7.5).

Variable	Test	Statistic	P Value
lengthRes	Shapiro-Wilk	.971	.773
lengthRes	Lilliefors (KS)	.089	.946
widthRes	Shapiro-Wilk	.951	.376
widthRes	Lilliefors (KS)	.157	.220
cwallRes	Shapiro-Wilk	.928	.139
cwallRes	Lilliefors (KS)	.126	.555

Figure 7.1: Normality tests (Shapiro-Wilkins and Kolmogorov-Smirnof) performed over the residuals of length (lengthRes), width (widthRes) and cell wall thickness (cwallRes) variables distributed normally ($P > 0.05$).

Variance Check

	Test	*P-Value*
Levene's	1.68985	0.2092

Variance Check

	Test	*P-Value*
Levene's	2.15564	0.1332

Variance Check

	Test	*P-Value*
Levene's	0.36221	0.7811

Figure 7.2: Levene's tests (homogeneity of variances) performed over the residuals of length (top left), width (top right) and cell wall thickness (bottom left) variables showed homogeneity of the variances ($P > 0.05$).

ANOVA Table for length by condition

Source	*Sum of Squares*	*Df*	*Mean Square*	*F-Ratio*	*P-Value*
Between groups	1101.11	3	367.037	2.40	0.1064
Within groups	2451.64	16	153.228		
Total (Corr.)	3552.75	19			

ANOVA Table for cwall by condition

Source	*Sum of Squares*	*Df*	*Mean Square*	*F-Ratio*	*P-Value*
Between groups	0.259999	3	0.0866663	0.39	0.7585
Within groups	3.51276	16	0.219548		
Total (Corr.)	3.77276	19			

ANOVA Table for width by condition

Source	*Sum of Squares*	*Df*	*Mean Square*	*F-Ratio*	*P-Value*
Between groups	12.5223	3	4.1741	0.40	0.7529
Within groups	165.785	16	10.3616		
Total (Corr.)	178.307	19			

Figure 7.3: p-values of ANOVA tests. Length (top left), width (top right) and cell wall thickness (bottom left).

Summary Statistics for length

condition	Count	Average	Standard deviation	Coeff. of variation
Control	5	66.723	13.1705	19.739%
Copper	5	60.3505	11.9368	19.7791%
Iron	5	71.408	16.3458	22.8908%
IronCopper	5	51.618	5.45664	10.5712%
Total	20	62.5249	13.6743	21.8702%

condition	Minimum	Maximum	Range	Stnd. skewness	Stnd. kurtosis
Control	53.6	85.975	32.375	0.557302	-0.134372
Copper	43.41	75.035	31.625	-0.308746	0.0504213
Iron	51.295	90.62	39.325	0.0635541	-0.891652
IronCopper	44.74	57.15	12.41	-0.483997	-1.16877
Total	43.41	90.62	47.21	1.22894	-0.300492

Summary Statistics for width

condition	Count	Average	Standard deviation	Coeff. of variation
Control	5	19.3756	4.62694	23.8802%
Copper	5	17.7995	0.792867	4.45444%
Iron	5	19.905	2.74187	13.7748%
IronCopper	5	18.652	3.44836	18.4879%
Total	20	18.933	3.06343	16.1803%

condition	Minimum	Maximum	Range	Stnd. skewness	Stnd. kurtosis
Control	15.023	26.605	11.582	0.936149	0.437061
Copper	16.415	18.41	1.995	-1.79733	1.88799
Iron	17.225	23.765	6.54	0.571259	-0.560497
IronCopper	14.8	22.625	7.825	0.0388195	-1.17881
Total	14.8	26.605	11.805	1.58561	0.581271

Summary Statistics for cwall

condition	Count	Average	Standard deviation	Coeff. of variation
Control	5	2.37574	0.461093	19.4084%
Copper	5	2.27885	0.493947	21.6753%
Iron	5	2.59096	0.369585	14.2644%
IronCopper	5	2.37942	0.53386	22.4366%
Total	20	2.40624	0.445608	18.5188%

condition	Minimum	Maximum	Range	Stnd. skewness	Stnd. kurtosis
Control	1.89	2.99625	1.10625	0.197566	-0.630771
Copper	1.72083	3.01337	1.29254	0.586909	0.189453
Iron	2.15667	3.17375	1.01708	0.862469	0.968733
IronCopper	1.84	3.20875	1.36875	0.969028	0.340425
Total	1.72083	3.20875	1.48792	0.627646	-0.679914

Figure 7.4: Summary statistics of each measured variable among the different conditions. Length (top left), width (top right) and cell wall thickness (bottom left).

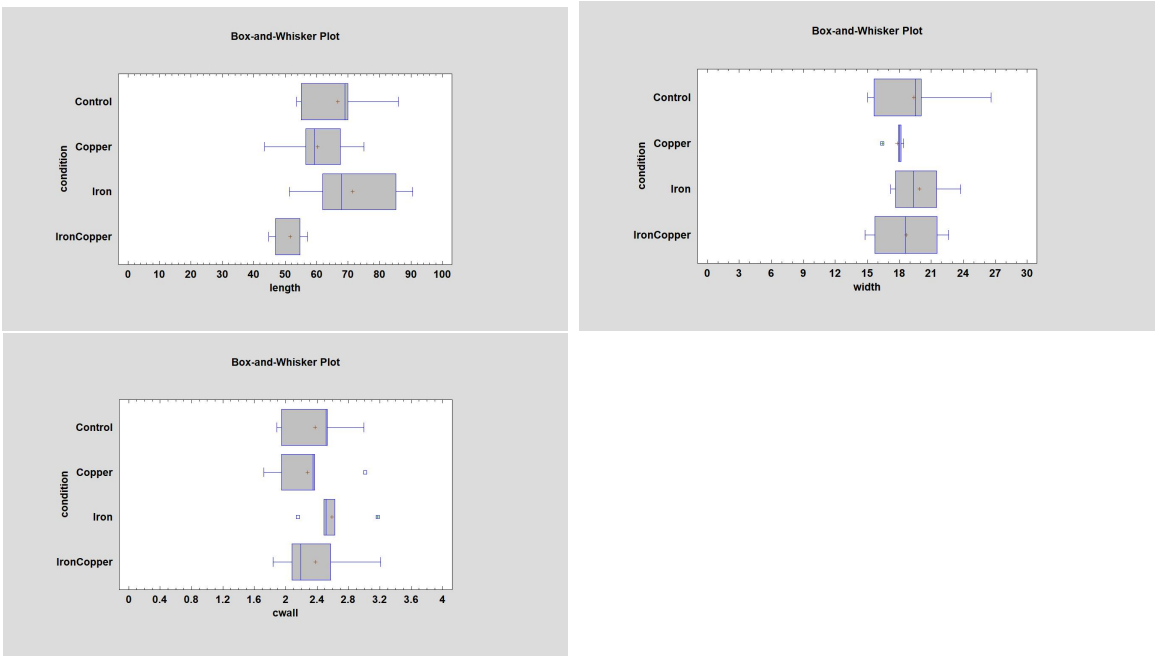

Figure 7.5: Box-whisker plots performed for each measured variable among the different conditions. Length (top left), width (top right), and cell wall thickness (bottom left).

7.2 Comparison between central and border cells variables inside each group.

7.2.1 Cells' lengths

Here we show that the central and border cells´ length measures of the 4 conditions (control, iron, copper and ironcopper) followed a normal distribution (fig. 7.6). In general, they showed homogeneous variances (except for iron and copper groups, fig. 7.7). Due to these 2 things, only parametric tests were performed, specifically, t-tests and ANOVA tests (only for the 2 cases with different variances). Here we also report the p-values of the tests (fig. 7.8) and summary statistics (fig. 7.9).

Variable	Test	Statistic	P Value
ControlCentral	Shapiro-Wilk	.942	.683
ControlCentral	Lilliefors (KS)	.219	.596
ControlBorder	Shapiro-Wilk	.979	.930
ControlBorder	Lilliefors (KS)	.165	.926
IronCentral	Shapiro-Wilk	.826	.129
IronCentral	Lilliefors (KS)	.243	.428
IronBorder	Shapiro-Wilk	.918	.517
IronBorder	Lilliefors (KS)	.227	.541
CopperCentral	Shapiro-Wilk	.994	.992
CopperCentral	Lilliefors (KS)	.137	.990
CopperBorder	Shapiro-Wilk	.940	.669
CopperBorder	Lilliefors (KS)	.232	.504
IroncopperCentral	Shapiro-Wilk	.988	.974
IroncopperCentral	Lilliefors (KS)	.161	.939
IroncopperBorder	Shapiro-Wilk	.845	.178
IroncopperBorder	Lilliefors (KS)	.258	.335

Figure 7.6: Normality tests (Shapiro-Wilkins and Kolmogorov-Smirnof) performed over the length measures of the 4 conditions (control, iron, copper and ironcopper), distributed normally ($P > 0.05$).

		Levene Statistic	df1	df2	Sig.
ControlLength	Based on Mean	5.231	1	8	.051
	Based on Median	3.573	1	8	.095
	Based on Median and with adjusted df	3.573	1	4.708	.121
	Based on trimmed mean	5.303	1	8	.050
IronLength	Based on Mean	7.292	1	8	.027
	Based on Median	6.858	1	8	.031
	Based on Median and with adjusted df	6.858	1	4.230	.056
	Based on trimmed mean	7.618	1	8	.025
CopperLength	Based on Mean	11.186	1	8	.010
	Based on Median	3.536	1	8	.097
	Based on Median and with adjusted df	3.536	1	4.439	.126
	Based on trimmed mean	10.759	1	8	.011
IroncopperLength	Based on Mean	.696	1	8	.428
	Based on Median	.298	1	8	.600
	Based on Median and with adjusted df	.298	1	5.764	.605
	Based on trimmed mean	.618	1	8	.455

Figure 7.7: Levene's tests (homogeneity of variances) performed over length measures of the 4 conditions (control, iron, copper and ironcopper). Only the iron and copper groups did not have homogeneous variances ($P < 0.05$).

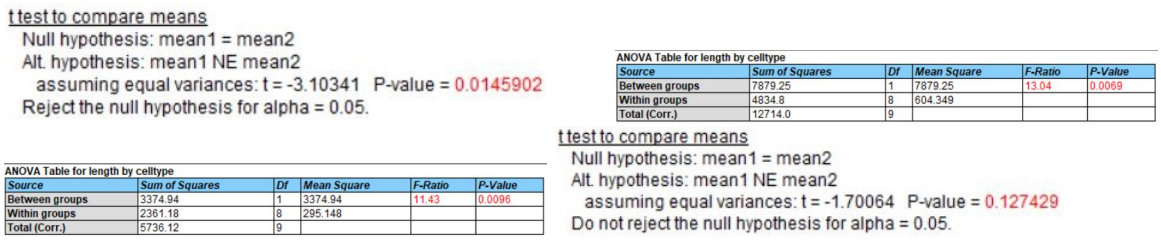

Figure 7.8: p-values of t (top left and bottom right) and ANOVA tests (top right and bottom left) over length measures. Control (top left), iron (top right), copper (bottom left) and ironcopper (bottom right).

Summary Statistics

	Clength	Blength
Count	5	5
Average	47.592	85.854
Standard deviation	7.10633	26.6369
Coeff. of variation	14.9318%	31.0258%
Minimum	39.21	53.01
Maximum	57.17	122.2
Range	17.96	69.19
Stnd. skewness	0.149287	0.160412
Stnd. kurtosis	-0.444929	-0.227645

Summary Statistics for length

celltype	Count	Average	Standard deviation	Coeff. of variation	Minimum
border	5	81.768	23.5203	28.7647%	50.39
central	5	45.026	6.0903	13.5262%	36.43
Total	10	63.397	25.2457	39.8216%	36.43

celltype	Maximum	Range	Stnd. skewness	Stnd. kurtosis
border	107.6	57.21	-0.43654	-0.770246
central	52.6	16.17	-0.309	0.0405138
Total	107.6	71.17	1.09945	-0.584524

Summary Statistics for length

celltype	Count	Average	Standard deviation	Coeff. of variation	Minimum
border	5	99.478	34.2166	34.3961%	52.68
central	5	43.338	6.15828	14.2099%	37.45
Total	10	71.408	37.5855	52.6349%	37.45

celltype	Maximum	Range	Stnd. skewness	Stnd. kurtosis
border	133.1	80.42	-0.349787	-0.630975
central	49.91	12.46	0.189201	-1.38017
Total	133.1	95.65	1.16461	-0.529391

Summary Statistics

	Clength	Blength
Count	5	5
Average	45.708	57.528
Standard deviation	8.09644	13.2659
Coeff. of variation	17.7134%	23.0598%
Minimum	34.56	46.65
Maximum	56.03	79.74
Range	21.47	33.09
Stnd. skewness	-0.148051	1.46356
Stnd. kurtosis	-0.0194555	1.19331

Figure 7.9: Summary statistics of length measures. Control (top left), iron (top right), copper (bottom left) and ironcopper (bottom right).

7.2.2 Cells' widths

Here we show that the central and border cells´ width measures of the 4 conditions (control, iron, copper, and ironcopper) followed a normal distribution (fig. 7.10). They also showed homogeneous variances (fig. 7.11). Due to these 2 things, only parametric tests were performed, specifically, t-tests. Here we also report the p-values of the tests (fig. 7.12) and summary statistics (fig. 7.13).

Variable	Test	Statistic	P Value
ControlCentral	Shapiro-Wilk	.837	.157
ControlCentral	Lilliefors (KS)	.278	.229
ControlBorder	Shapiro-Wilk	.928	.586
ControlBorder	Lilliefors (KS)	.205	.696
IronCentral	Shapiro-Wilk	.835	.152
IronCentral	Lilliefors (KS)	.292	.171
IronBorder	Shapiro-Wilk	.889	.353
IronBorder	Lilliefors (KS)	.250	.381
CopperCentral	Shapiro-Wilk	.914	.489
CopperCentral	Lilliefors (KS)	.230	.520
CopperBorder	Shapiro-Wilk	.915	.498
CopperBorder	Lilliefors (KS)	.286	.196
IroncopperCentral	Shapiro-Wilk	.901	.418
IroncopperCentral	Lilliefors (KS)	.242	.435
IroncopperBorder	Shapiro-Wilk	.912	.480
IroncopperBorder	Lilliefors (KS)	.253	.364

Figure 7.10: Normality tests (Shapiro-Wilkins and Kolmogorov-Smirnof) performed over the width measures of the 4 conditions (control, iron, copper and ironcopper), distributed normally ($P > 0.05$).

		Levene Statistic	df1	df2	Sig.
ControlWidth	Based on Mean	3.904	1	8	.084
	Based on Median	1.732	1	8	.225
	Based on Median and with adjusted df	1.732	1	5.616	.239
	Based on trimmed mean	3.612	1	8	.094
IronWidth	Based on Mean	.557	1	8	.477
	Based on Median	.111	1	8	.748
	Based on Median and with adjusted df	.111	1	7.704	.748
	Based on trimmed mean	.581	1	8	.468
CopperWidth	Based on Mean	.511	1	8	.495
	Based on Median	.443	1	8	.524
	Based on Median and with adjusted df	.443	1	7.708	.525
	Based on trimmed mean	.540	1	8	.484
IroncopperWidth	Based on Mean	.040	1	8	.846
	Based on Median	.010	1	8	.925
	Based on Median and with adjusted df	.010	1	7.999	.925
	Based on trimmed mean	.045	1	8	.837

Figure 7.11: Levene's tests (homogeneity of variances) performed over width measures of the 4 conditions (control, iron, copper and ironcopper) showed homogeneous variances ($P > 0.05$) between border and central cells.

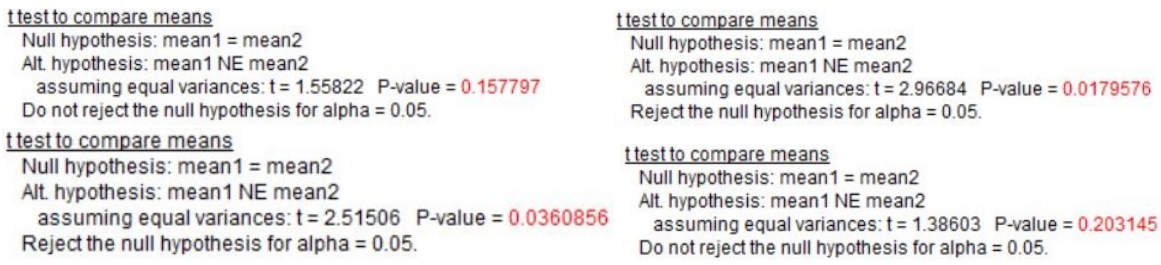

Figure 7.12: p-values of t tests over width measures. Control (top left), iron (top right), copper (bottom left) and ironcopper (bottom right).

Summary Statistics

	Cwidth	Bwidth
Count	5	5
Average	22.208	16.5432
Standard deviation	3.06218	7.53024
Coeff. of variation	13.7886%	45.5186%
Minimum	19.05	9.256
Maximum	25.61	27.84
Range	6.56	18.584
Stnd. skewness	0.381308	0.823628
Stnd. kurtosis	-1.36068	-0.0731807

Summary Statistics

	Cwidth	Bwidth
Count	5	5
Average	24.022	15.788
Standard deviation	4.60988	4.15471
Coeff. of variation	19.1903%	26.3156%
Minimum	19.08	8.97
Maximum	29.15	19.63
Range	10.07	10.66
Stnd. skewness	-0.287852	-1.28463
Stnd. kurtosis	-1.25561	0.991218

Summary Statistics

	Cwidth	Bwidth
Count	5	5
Average	20.298	15.518
Standard deviation	3.39032	2.56247
Coeff. of variation	16.7027%	16.5129%
Minimum	16.07	12.07
Maximum	23.82	18.32
Range	7.75	6.25
Stnd. skewness	-0.09728	-0.48435
Stnd. kurtosis	-1.01953	-0.747119

Summary Statistics

	Cwidth	Bwidth
Count	5	5
Average	20.258	17.046
Standard deviation	3.63013	3.69783
Coeff. of variation	17.9195%	21.6933%
Minimum	14.82	13.02
Maximum	23.55	21.7
Range	8.73	8.68
Stnd. skewness	-0.875097	0.379464
Stnd. kurtosis	-0.176656	-1.04448

Figure 7.13: Summary statistics of width measures. Control (top left), iron (top right), copper (bottom left) and ironcopper (bottom right).

7.2.3 Cells' wall thickness

Here we show that the central and border cells´ walls thickness measures of the 4 conditions (control, iron, copper and ironcopper) followed a normal distribution (fig. 7.14). In general, they showed homogeneous variances (except for iron and copper groups, fig. 7.15). Due to these 2 things, only parametric tests were performed, specifically, t-tests and ANOVA tests (only for the 2 cases with different variances). Here we also report the p-values of the tests (fig. 7.16) and summary statistics (fig. 7.17).

Variable	Test	Statistic	P Value
ControlCentral	Shapiro-Wilk	.841	.167
ControlCentral	Lilliefors (KS)	.292	.172
ControlBorder	Shapiro-Wilk	.887	.343
ControlBorder	Lilliefors (KS)	.220	.590
IronCentral	Shapiro-Wilk	.884	.325
IronCentral	Lilliefors (KS)	.290	.181
IronBorder	Shapiro-Wilk	.976	.912
IronBorder	Lilliefors (KS)	.178	.870
CopperCentral	Shapiro-Wilk	.906	.443
CopperCentral	Lilliefors (KS)	.283	.209
CopperBorder	Shapiro-Wilk	.815	.106
CopperBorder	Lilliefors (KS)	.335	.069
IroncopperCentral	Shapiro-Wilk	.864	.244
IroncopperCentral	Lilliefors (KS)	.289	.183
IroncopperBorder	Shapiro-Wilk	.972	.885
IroncopperBorder	Lilliefors (KS)	.197	.753

Figure 7.14: Normality tests (Shapiro-Wilkins and Kolmogorov-Smirnof) performed over the cell wall thickness measures of the 4 conditions (control, iron, copper and ironcopper), distributed normally ($P > 0.05$).

		Levene Statistic	df1	df2	Sig.
ControlCwall	Based on Mean	.070	1	8	.798
	Based on Median	.097	1	8	.763
	Based on Median and with adjusted df	.097	1	7.171	.764
	Based on trimmed mean	.073	1	8	.794
IronCwall	Based on Mean	.000	1	8	1.000
	Based on Median	.006	1	8	.940
	Based on Median and with adjusted df	.006	1	7.643	.940
	Based on trimmed mean	.000	1	8	.992
CopperCwall	Based on Mean	3.176	1	8	.113
	Based on Median	.538	1	8	.484
	Based on Median and with adjusted df	.538	1	5.747	.492
	Based on trimmed mean	2.896	1	8	.127
IroncopperCwall	Based on Mean	.533	1	8	.486
	Based on Median	.268	1	8	.619
	Based on Median and with adjusted df	.268	1	7.949	.619
	Based on trimmed mean	.538	1	8	.484

Figure 7.15: Levene's tests (homogeneity of variances) performed over cell wall thickness measures of the 4 conditions (control, iron, copper and ironcopper) showed homogeneous variances ($P > 0.05$) between central and border cells.

t test to compare means
Null hypothesis: mean1 = mean2
Alt. hypothesis: mean1 NE mean2
assuming equal variances: t = 0.0661496 P-value = 0.948882
Do not reject the null hypothesis for alpha = 0.05.

t test to compare means
Null hypothesis: mean1 = mean2
Alt. hypothesis: mean1 NE mean2
assuming equal variances: t = -1.62061 P-value = 0.143761
Do not reject the null hypothesis for alpha = 0.05.

t test to compare means
Null hypothesis: mean1 = mean2
Alt. hypothesis: mean1 NE mean2
assuming equal variances: t = -2.05794 P-value = 0.0735948
Do not reject the null hypothesis for alpha = 0.05.

t test to compare means
Null hypothesis: mean1 = mean2
Alt. hypothesis: mean1 NE mean2
assuming equal variances: t = -2.8277 P-value = 0.0222287
Reject the null hypothesis for alpha = 0.05.

Figure 7.16: p-values of t tests over cell wall thickness measures. Control (top left), iron (top right), copper (bottom left) and ironcopper (bottom right) between central and border cells.

Summary Statistics

	Ccwall	Bcwall
Count	5	5
Average	2.38765	2.36383
Standard deviation	0.537502	0.59937
Coeff. of variation	22.5118%	25.3558%
Minimum	1.9425	1.7725
Maximum	3.1275	3.09
Range	1.185	1.3175
Stnd. skewness	0.697205	0.240319
Stnd. kurtosis	-0.908801	-1.20137

Summary Statistics

	Ccwall	Bcwall
Count	5	5
Average	2.37742	2.8045
Standard deviation	0.445312	0.385934
Coeff. of variation	18.7309%	13.7612%
Minimum	1.955	2.24
Maximum	3.1	3.2475
Range	1.145	1.0075
Stnd. skewness	1.17929	-0.578171
Stnd. kurtosis	0.889839	0.0280614

Summary Statistics

	Ccwall	Bcwall
Count	5	5
Average	1.84845	2.55845
Standard deviation	0.390114	0.665547
Coeff. of variation	21.1049%	26.0137%
Minimum	1.395	2.04667
Maximum	2.4695	3.55725
Range	1.0745	1.51058
Stnd. skewness	0.927015	0.973556
Stnd. kurtosis	1.05833	-0.299017

Summary Statistics

	Ccwall	Bcwall
Count	5	5
Average	1.87967	2.87917
Standard deviation	0.507651	0.605793
Coeff. of variation	27.0075%	21.0406%
Minimum	1.43	2.1725
Maximum	2.71	3.7075
Range	1.28	1.535
Stnd. skewness	1.25016	0.381289
Stnd. kurtosis	0.948096	-0.454321

Figure 7.17: Summary statistics of cell wall thickness measures. Control (top left), iron (top right), copper (bottom left) and ironcopper (bottom right).

7.3 Pseudoreplication

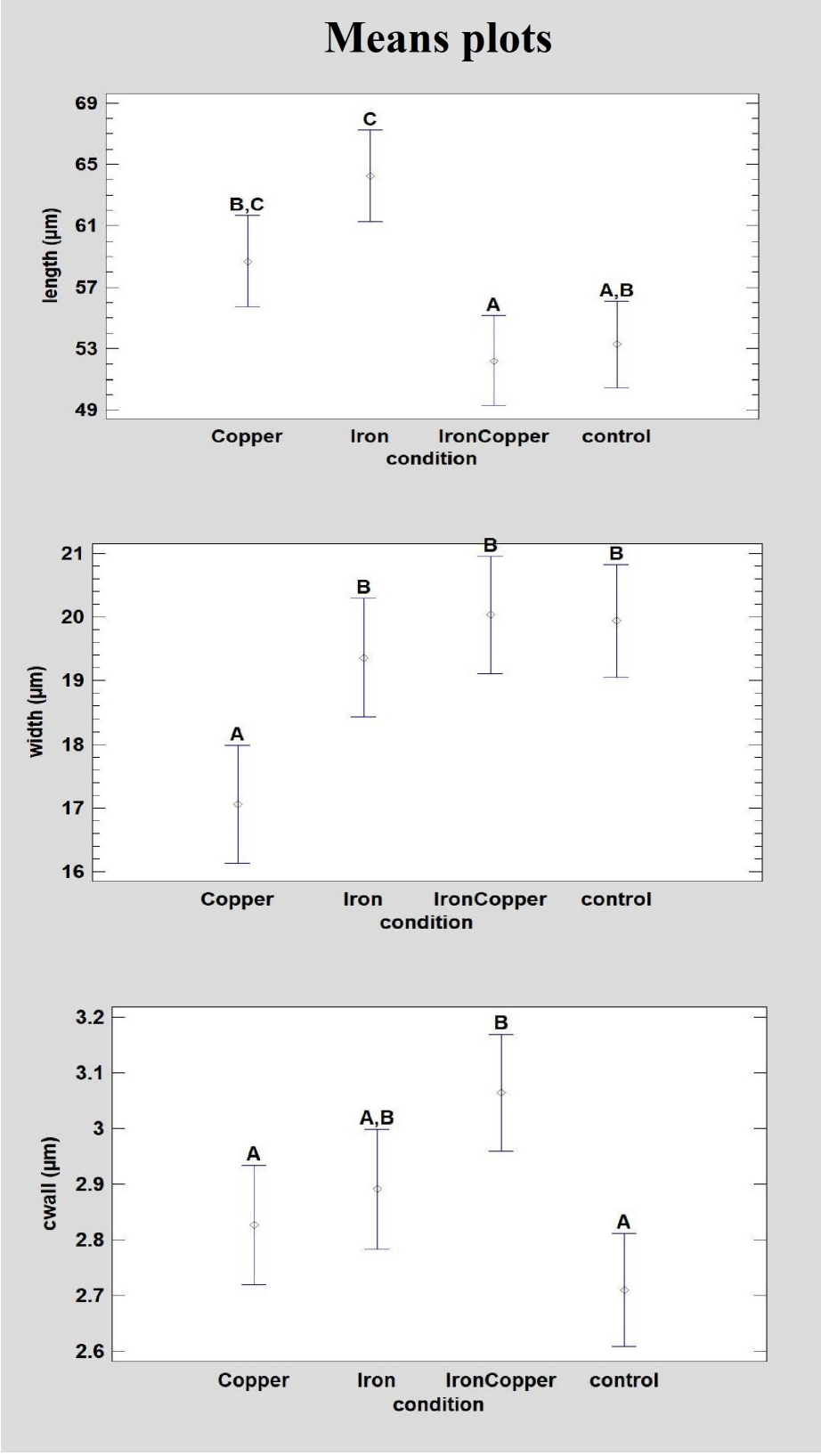

Figure 7.18: Mean plots of the ANOVA tests for the first statistical model (with pseudoreplication). Length (top), width (central) and cell wall thickness (bottom).

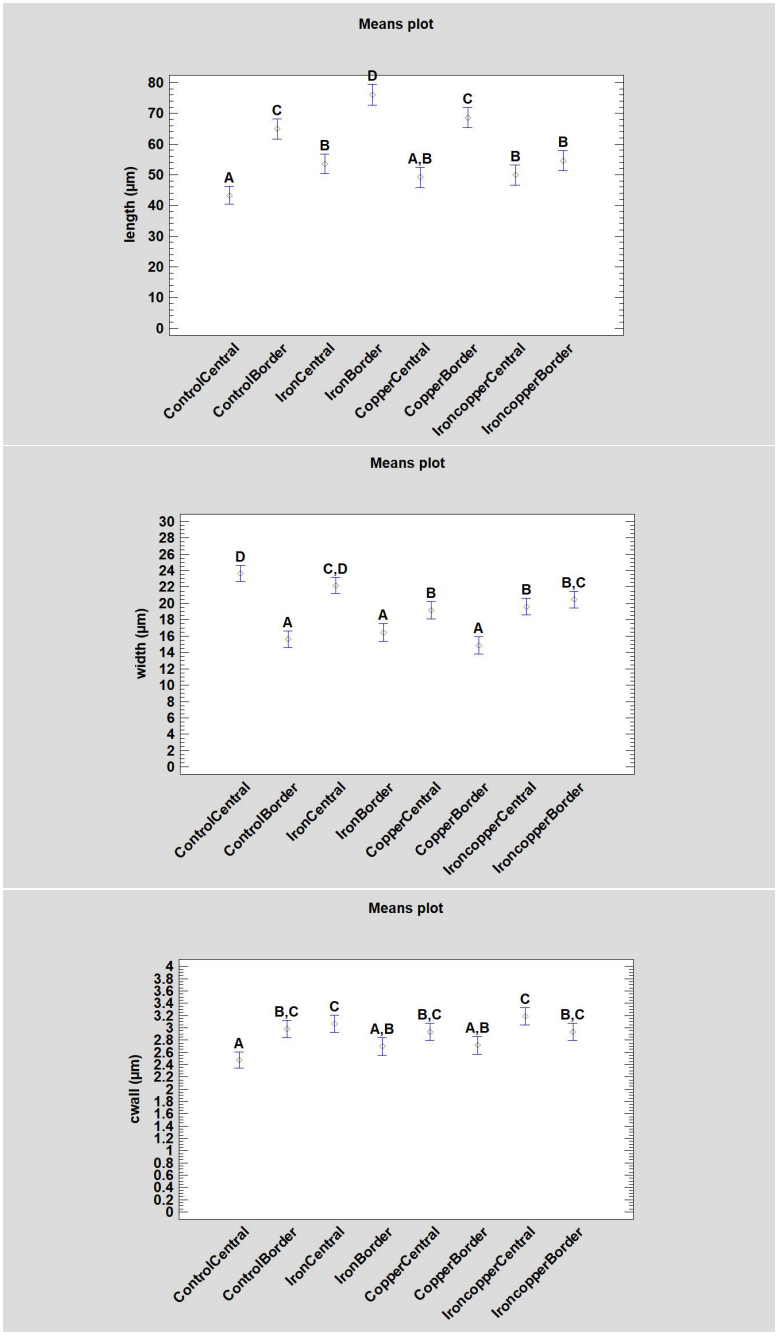

Figure 7.19: Means plots of the ANOVAs tests, of the first statistical model (with pseudoreplication) between central and border cells for the first statistical model for the three variables. Length (top), width (central) and cell wall thickness (bottom).